International Journal of Aquatic Science
ISSN: 2008-8019
Vol 12, Issue 02, 2021

Study Of Electron Transport Coefficients And Critical Field Strength In N_2O And N_2O-SF_6 Mixtures Using Boltzmann Equation Analysis

Mohammad Mustafa Othman[1], Gullala YasenBakr[2], Sherzad Aziz Taha[3]

[1,2,3]*Department of Physics, College of education, University of Salahaddin-Hawler, KRG, Iraq*
[1]*Department of Library Science, Tishik International university, KRG, Erbil*

Email id: [1]muhamad.othman@su.edu.krd

Abstract
equation over the density-normalized electric field strength, E/N from 0.1 to 1000 Td ($1Td=10^{-17}$ $V.cm^2$). The swarm parameters such as, drift velocity, electron mean energy, characteristic energy, ionization and attachment coefficients were analyzed using a set of cross sections for the gases. The density-reduced effective ionization coefficient $(\alpha - \eta)/N$ has also been calculated.The present results agree well with previous experimental and theoretical results. Moreover, the E/N value at which ionization coefficient equals attachment coefficient, the critical field strength was calculated to be $(E/N)_{cr}$=199 Td for pure N_2O gas, which is lower than that of pure SF_6 gas (361 Td), a widely used as insulating gas. In addition, it's found that the critical field strength (voltage breakdown) increase with increasing SF_6 concentration in the gas mixtures.

Keywords: Nitrous oxide, swarm parameters, cross section, critical field strength, breakdown voltage, EEDF.

1. INTRODUCTION

Nitrous oxide (N_2O) is an electronegative gaswith breakdown voltage about half that of SF_6 (Biasiutti, 2013), has excellent insulation widely used in gas insulated transmission line and gas insulated switchgear. Nitrous oxide known as laughing gas with a low global warming potential after carbon dioxide and methane. N_2O is atmospheric greenhouse gas withhigh global warming potential (GWP) is310times higher than that of CO_2(as a reference, the GWP of CO_2=1) and the life time is 120 years in the atmosphere on 100 year horizon (Gunnar Myhre et al., 2013). The concentration of nitrous oxide reached (333 ppb) in 2020 is much lower than that of CO_2 and CH_4,.

Nitrous oxide is a gas at room temperature, is 1.53 times denser than air, 34 times more soluble than nitrogen in blood, is colorless, tasteless, non-flammable, odorless, non-toxic and ozone depleting substance. N_2O has stable chemical structures has a low boiling point of -88:5 C, and strong electrical insulation gas use in numerous applications, chemistry, medicine, media gas laser, plasma etching, high-voltage equipment, thin film by using plasma enhanced chemical vapourdeposition and technology.Besides the GWP of N_2O is lower than that of SF_6, it has been suggested as a potential replacement to SF_6 gas which used in the electrical industry with an higherglobal warming potential 23900 times higher than that of CO_2, and with long life time in atmosphere 3400 years (Kim, et al., 2004), and would allow

application at higher pressures than that SF_6. In 1997 the Kyoto protocol has listed SF_6, CO_2, CH_4, N_2O and hydrofluorocarbon as strong greenhouse gases, and for environment required to reduce the use of this gases.

Electron swarm parameters is described by the following parameters: the electron drift velocity v_d, mean electron energy <ε>, characteristic energy D/μ_e (where D is diffusion coefficient and μ_e electron mobility), reduced ionization coefficient α/N, reduced attachment coefficient η/N. These swarm parameters have been measured in pure N_2O for small values of the reduced electric field E/N< 490 Td (1Td=10^{-17} V cm^2), (Mechlinska-Drewko, 2003).
The drift velocity in pure N_2O was measured by (Lisovskiy, et al., 2006) in strong electric field from RF breakdown curves in the range E/P varying from 87 to 840 $Vcm^{-1}Torr^{-1}$.The electron drift velocity and effective ionization coefficients in N_2O, N_2O-N_2 and N_2O-SF_6 mixtures are measured by (Basurto, et al., 2007) over E/N varying from 0.5 to 400 Td. (Dupljanin, et al., 2010) measured the electron transport coefficients and electron collision cross sections in N_2O and in N_2O-N_2 mixtures.Recently the electron swarm coefficients and the limiting field strength of binary gas mixtures SF_6-N_2O measured by (Basurto, et al., 2013) with a pulsed Townsend technique over a wide range of E/N from 130 to 420 Td.Furthermore, one recent review (Andreas, et al., 2020) states that still relatively little is known on electron swarm parameters and ionization and attachment properties,and electrical insulation properties for this molecule.Finally, (Hainan Liu, 2020), studied the electron scattering with N_2O molecule for control and reduction of atmospheric pollution.
In the present work we calculated the electron swarm parameters, effective ionization coefficients and critical fieldstrength for N_2O, SF_6 and different mixtures (5%, 20% and 80%) of SF_6, by using two-term solution of the Boltzmann equation method, over a wide range of the reduced electric field strength E/N from 0.1 to 1000 Td, where E is the electric field and N is the gas density.

2. THEORETICAL FORMULATION

In this section we summarize the theoretical expression actually used in our calculation.
The electron energy distribution function *f(ε)* is obtained from the two-term solution of the Boltzmann equation(Colonna & D'Angola, 2016). The electron energy distribution function can be normalized.

$$\int_0^\infty f(\varepsilon)\sqrt{\varepsilon}d\varepsilon = 1 \quad (1)$$

The Boltzmann equation for electrons moves due to an external (dc) electric field $\overline{E}$ is written as (Smith and Thomson, 1974; Phelps and Pitchford, 1982; Othman, et al., 2019),

$$\frac{\partial f(v)}{\partial t} + v.\nabla_r f(v) - \frac{e}{m}\overline{E}.\nabla_v f(v) = \left(\frac{\partial f}{\partial f}\right)_{oll} \quad (2)$$

Where, e is electron charge, m is the electron mass, the right part of the equation denotes the rate of change in the electron distribution due to elastic and inelastic collisions. To solve the Boltzmann transport equation the electron distribution function is expanded in two terms of Legendre polynomials, $f(\overline{v}) = f_o(v) + f_1(v)\cos\theta$, where $f_o(v)$ is the isotropic and $f_1(v)$ is anisotropic part of the distribution function where $f_1(v) << f_o(v)$. The expansions in

spherical harmonic using two term solution have been given elsewhere (Govinda-Raju, G. 2006).

The electron swarm parameters are expressed in term of the electron energy distribution function *f(ε)* and collisioncross sections $Q_m^T(\varepsilon)$ as follows

The electron drift velocity is,

$$v_d = -\frac{\overline{E}}{3}\sqrt{\frac{2e}{m}}\int_0^\infty \frac{\varepsilon}{NQ_m^T(\varepsilon)}\frac{\partial f(\varepsilon)}{\partial \varepsilon}d\varepsilon \qquad (3)$$

The electron mean energy is,

$$\langle \varepsilon \rangle = \int_0^\infty \varepsilon^{3/2} f(\varepsilon) d\varepsilon \qquad (4)$$

The reduced transverse diffusion coefficient is,

$$D_T N = \frac{1}{3}\sqrt{\frac{2e}{m}}\int_0^\infty \frac{\varepsilon}{Q_m^T(\varepsilon)} f(\varepsilon) d\varepsilon \qquad (5)$$

The reduced electron mobilityis,

$$\mu_e N = -\frac{1}{3}\sqrt{\frac{2e}{m}}\int_0^\infty \frac{\varepsilon}{Q_m^T(\varepsilon)}\frac{\partial f(\varepsilon)}{\partial \varepsilon}d\varepsilon \qquad (6)$$

The characteristic energy is,

$$\varepsilon_k = \frac{eD_T}{\mu_e} \qquad (7)$$

The values of electron energy distribution function *f(ε)* are calculated from Boltzmann equation using all the electron collision cross sections as follows,

$$Q_m^T(\varepsilon) = Q_m(\varepsilon) + \sum_j Q_e(\varepsilon) + Q_i(\varepsilon) + Q_a(\varepsilon) \qquad (8)$$

Here, $Q_m^T(\varepsilon)$ represented the total effective momentum transfer cross section, The cross sections $Q_m(\varepsilon)$, $Q_k(\varepsilon)$, $Q_i(\varepsilon)$ and $Q_a(\varepsilon)$ are indicate the momentum transfer, excitation (vibration and electronic), ionization, and attachment, respectively.

The reduced ionization coefficient is (Tuan, 2014, 2016),

$$\frac{\alpha}{N} = \frac{1}{v_d}\sqrt{\frac{2e}{m}}\int_i^\infty Q_i(\varepsilon) f(\varepsilon)\varepsilon d\varepsilon \qquad (9)$$

The reduced attachment coefficient is,

$$\frac{\eta}{N} = \frac{1}{v_d}\sqrt{\frac{2e}{m}}\int_a^\infty Q_a(\varepsilon) f(\varepsilon)\varepsilon d\varepsilon \qquad (10)$$

Where, $Q_i(\varepsilon)$, $Q_a(\varepsilon)$ are ionization and attachment cross section, here, i and a is the ionization and attachment threshold energy. The reduced critical electric field strength $(E/N)_{cr}$is calculated when the formation and loss electrons reach a balance, this mean that the effective ionization equal to zero (Zhao, et al., 2013).

$$\overline{\alpha} = \frac{\alpha}{N} - \frac{\eta}{N} = \frac{\alpha - \eta}{N} = 0 \qquad (11)$$

3. COLLISION CROSS SECTION

To apply the Boltzmann equation analysis, the electron energy distribution function (EEDF) and values of transport coefficients in nitrous oxide (N_2O) gas are calculated from the

knowledge of electroncollisioncross section (elastic and inelastic) which reported by. This sets includes 9 collisional processes: one momentum-transfer cross section (Q_m), three vibration excitation (Q_{v1}, Q_{v2} and Q_{v3}) with threshold energy 0.073, 0159, and 0.276 eV respectively and three electronic excitation (Q_{ex}) cross section with threshold energy of 4.05, 8.5 and 9.6 eV, one dissociative attachment cross section (Q_a), and one ionization cross section (Q_i) with threshold energy 12.89 eV.
For$SF_6$the cross sections are, momentum transfer cross section Q_m was taken, while the sets of vibration excitation cross sections Q_v with threshold energy 0.095eV was taken from. The ionization cross sections having onset energy 15.8eV is taken from, electron excitation cross section Q_{ex} estimated from. The electron attachment cross sections Q_a are used in the calculation, for low energy $E \leq 0.140eV$ is estimated the measurements of, the value for $E > 0.14eV$ is taken from measurements.

4. RESULTS AND DISCUSSION

Many previous papers concentrated on the investigations of EEDF, electron swarm parameters of pure N_2O, and SF_6, at temperature300 K and pressure 1 atm. This paper also calculated thedensity-reduced effective ionization coefficient $(\alpha - \eta)/N$ and the density-normalized critical field strength $(E/N)_{cr}$ of N_2O-SF_6 mixtures using the cross section data reported in section 3.

The influence of the electron distribution function (EEDF) as a function of the mean electron energy for different ratio of reduced electric field (E/N) in N2O gas, is shown in figure 1. Clearly, the electron energy distribution function is strongly affected by changing the parameter E/N, subsequently the electron transport coefficients depends on the ratio E/N. Near the thresholds of the inelastic processes, the formation of the EEDF is strongly influenced by the electric field, which heats the electron component and thus increases the energy of the cold electrons. For electron energies in the range less than 2 eV, the EEDF decreases as the E/N increases, however for electron energies greater than 2eV the EEDF increases with increasing E/N, because at high value of E/N the kinetic energy of electrons increases. It is obviously appears from the figure that applying a high electric field (or E/N) leads to the development of EEDF to a higher energy tail.
Figure 2 is shown the influence of superelastic collisions on EEDF at reduced electric field strength 0.5, 5 and 30 Td with and without superelastic collision. It can be seen that superelastic collisions are effect the EEDF at low reduced electric field strength E/N, but are not important at high E/N values. For high values of reduced electric field strength E/N, the electrons gain their energy from the applied d.c electric field. The study of the influence of second kind (superelastic) collisions was explained in literatures of (Pietanza, et al., 2016; Pietanza, et al., 2016a).

Figure 3 shows the EEDF in pure N_2O, SF_6 and 50%N_2O-50%SF_6 gas mixtures under gas temperature of 300 K and E/N of 100 Td. It can be seen from the figure that the number of electrons in the low-energy region (electron energy less than 2 eV) increased but the number of high-energy electrons decreased. This is mainly due to the fact that N_2O is kind of strong electronegative gas, at low energy region larger amount of electrons were adsorbed and accumulated in pure N_2O gas.
Figure 4 shows the mean electron energy from 0.025 eV at E/N=0.1 Td to 13. 5 eV at E/N=1000 Td, at high E/N the mean electron energy sensitive to inelastic collisions. The variation of mean electron energy is progressive exponential, the electron gain all energies from the applied electric field. Comparison has been made with the theoretical values of and experimental values of (Mechlinska-Drewko, et al., 2003; Lisovskiy, et al., 2006) a good

agreement has been observed.The results of electron drift velocity in N_2O as a function of E/N is shown in figure 5, which increases with increasing E/N values, the results are compare with the theoretical values of and experimental values of (Dupljanin, et al., 2010; Basurto, et al., 2013). The agreement is good over the entire reduced electric field strength E/N range, on the other hand the theoretical results of, and experimental results of (Basurto, et al., 2013) are litle higher than present calculation.Figure 6 shows the calculated results for the electron drift velocity in SF6 as a function of E/N, in comparison with the experimental data of (Aschwanden, 1985; Lisovskiy, et al., 2010) as well as the theoretical results of (Wei, et al., 2014; Miric, et al., 2016; Seasa, et al., 2019), good agreements has been observed.On the other hand the experimental results of (Lisovskiy, et al., 2010),throughout the whole range of 90Td≤E/N≤200 Td is higher than the present calculation.Figure 7 gives the electron drift velocities, calculated in this work for 100% N_2O, 100%SF_6 and 50%N_2O-50%SF_6 mixture as a function of the *E*/*N*. It can be clearly observed at fixed value of E/N that the electron drift velocity displays a quick trend to increase as the N_2O content increases, especially in the low *E*/N range.

The characteristic energy in pure N_2O as a function of E/N is shown in figure 8. The present calculation were found in good agreement with experimental results of (Mechlinska-Drewko, 2003; Dupljanin, et al., 2010).

Figure 9, shows the calculated results for the normalized reduced ionization coefficient α/N as a function of E/N, in comparison with the experimental data of (Lisovskiy, et al., 2006) as well as the theoretical results of(Dupljanin, et al., 2010). Throughout the whole range of 70 Td≤E/N≤1000 Td good agreements has been observed. For E/N<350 Td, the experimental results of lower compare with the present results. In addition, the experimental results of (Lisovskiy, et al., 2006) over the range of E/N< 250 Td higher than present results.Figure 10 shows the comparison of the calculated normalized density attachment coefficient η/N in pure N_2O with the previous literatures (Lisovskiy, et al., 2006; Dupljanin, et al., 2010). A deviation between the calculated and experimental data of Yoshida, et al., 1999; Lisovskiy, et al., 2006) can be observed due to the cross-sections for the attachment, However, the calculated results show good agreement with theoretical results of (Dupljanin, et al., 2010) at room temperature, and experimental results.

In the present study, the results from the two-term approximation Boltzmann equation analysis and the data from the experimental measurements (Basurto, et al., 2007; Basurto, et al., 2013)and theoretical calculation (Dupijanin, et al., 2010) of the density-reduced effective ionization coefficient in pure N_2O are compared in Fig. 11. It can be observed that the density normalized coefficient $(\alpha - \eta)/N$ increases with increasingly reducing the field strength. Although the experimental results of is lower than present calculation over the range of E/N<90 Td.The density-normalized critical field strength $(E/N)_{cr}$ values at which ionization coefficient balance with attachment coefficient (α/N=η/N) is obtained in the present calculation is equal to approximately 199Td.

In figure 12 we show variation of the gas density reduced ionizationα/Nand attachment coefficientη/Nwith E/N for electrons in SF_6, by using the two–term Boltzmann equation analysis, which theoretical and experimental values for comparison are mention in the figure. It is seen that the ionization coefficient increase and attachment coefficient decreases as reduced electric field strength E/N increases. The attachment coefficient is defined the probability that an electron will attach to a gas molecule in traveling a unit distance in the electric field direction is a function of E/N. The agreement between the present calculation and previous experimental values of ,and theoretical results of (Abderrahmane and Lahouaria, 2005; Miric, et al., 2016) are excellent for ionization coefficient, on the other hand the

theoretical results ofItoh higher than that of present results for the range of E/N<215 Td by %7.

A zero value of (α-η)/N means a critical breakdown voltage of a gas, and the critical field strength $(E/N)_{cr}$ of the pure and binary mixture was calculated as the value of reduced electric field strength at (α-η)/N=0, and the critical electric field strength E_{cr} was then calculated by multiplying $(E/N)_{cr}$ by N, where N is the gas density of the gas.Figure 13 show the density normalized effective ionization coefficient (α-η)/N in SF_6 calculated over a range of E/N values from 100Td-700Td by using two-term solution of Boltzmann equation. The critical field strength$(E/N)_{cr}$ values at which (α/N=η/N) is obtained in the present calculation is equal to 361Td, in agreement with the experimental results of: 361Td, 361 Td (Xiao et al., 2000), 361 Td (Li, et al., 2012), 360Td Gonzalez-Magaña, et al., 2020), and theoretical results of: 362 Td , 360 (Tezcan, et al., 2010), 361 (Wei, et al.,2014), 361 (Mirić, et al., 2016). The effective ionization coefficient is almost zero, since ionizing collisions are balanced by attaching collisions, and for E/Nvalues smaller than the (E/N_{cr}, attachment processes become dominant, yielding negative values for the effective ionization coefficient as E/Nis decreased and; on the other hand, for *E/N* values above the $(E/N)_{cr}$, the effective ionization coefficient increases with increasing E/N valueswhere the ionization collisions become dominant and the effect of the attachment processes is not significant.

The linear relationship between the density-reduced effective ionization coefficient (α − η)/N and reduced electric field strength E/N is common for electronegative gases, such as SF6 and SF6 mixtures (Christophorou and Brunt, 2002). The law is verified valid for N_2O-SF_6 mixtures it can be represented by, $[(\alpha - \eta)/N](10^{-17}\ cm^2) = \beta[(E/N)-(E/N)_{cr}]$, where $(E/N)_{cr}$ is the critical field strength value, and β is the slope of the curve $(\alpha - \eta)/N = f(E/N)$ .The values of β and $(E/N)_{cr}$ depend on the content of SF_6 in the mixtures.which are shown in figure 14.The density-reduced effective ionization coefficient (α − η)/N increase with increasing reduced field strength E/N, and the critical field strength $(E/N)_{cr}$ of N_2O-SF_6 mixture increase with increasing SF_6molar fraction in the gas mixture.

The values of density-normalized critical electric field strength$(E/N)_{cr}$ are presented in Figure 15 as a function of N_2O content in the binary mixtures of SF_6 as a parameter with concentrations of 5%, 20% and 50%. The density-normalized critical electric field strength of the binary mixture N_2O-SF_6increases with increasing concentration of SF_6.

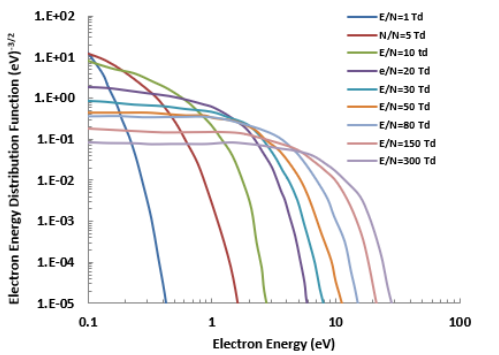

Figure 1. Electron energy distributions for swarms in N2O.

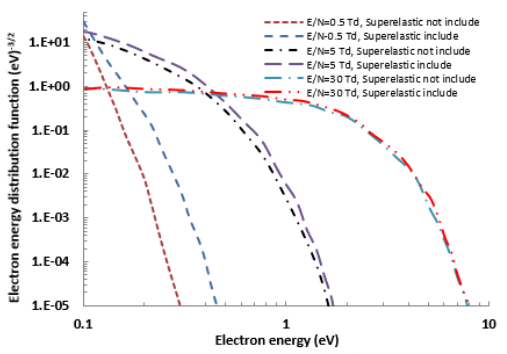

Figure 2. Electron energy distribution function in N_2O for E/N= 0.5, 5 and 30 Td, with and without the super-elastic process.

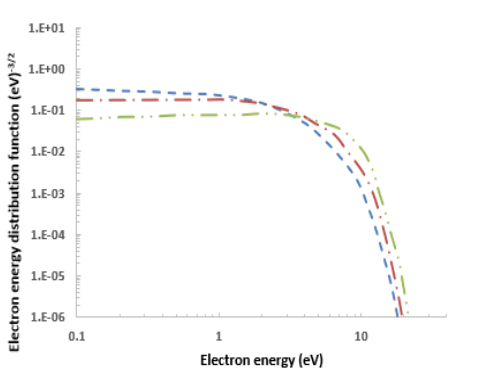

Figure 3. The electron energy distribution function for E/N=100 Td in pure N_2O, N_2O-SF_6 and SF_6.

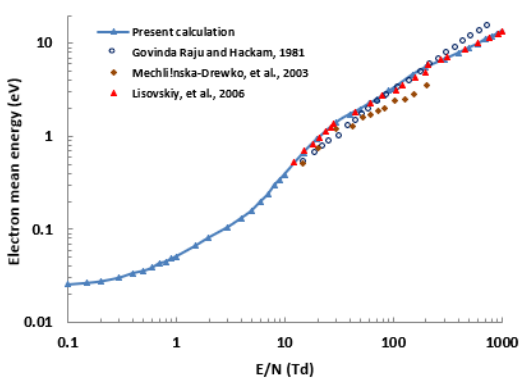

Figure 4. Electron mean energy <ε> in pure N_2O.

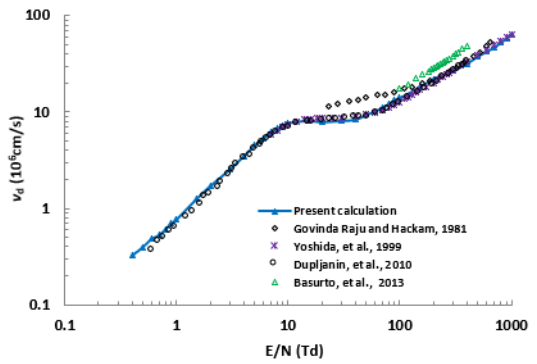

Figure 5. Electron drift velocity v_d in N_2O.

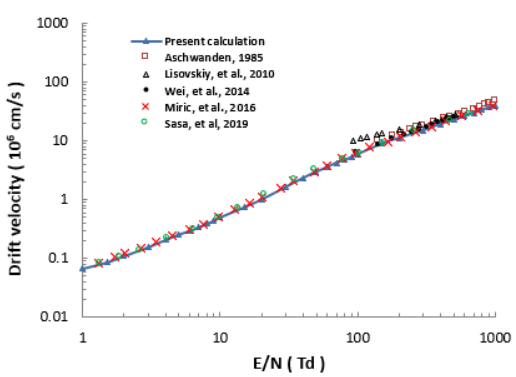

Figure 6 . Electron drift velocity in pure SF_6

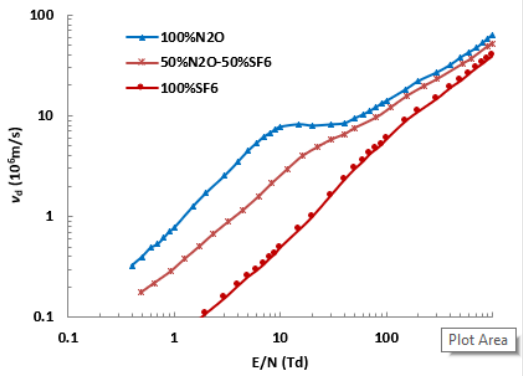

Figure 7. Electron drift velocity in 100%N_2O, 100%SF_6, and 50%N_2O-50%SF_6.

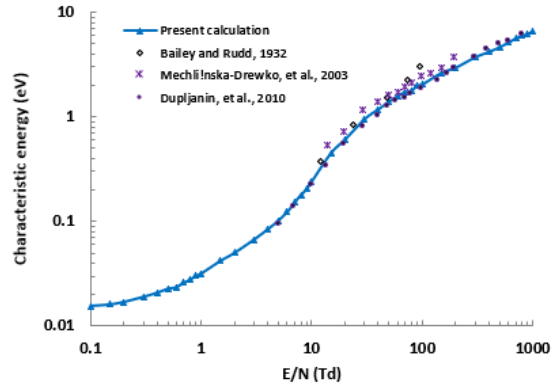

Figure 8. Characteristic energy in N_2O.

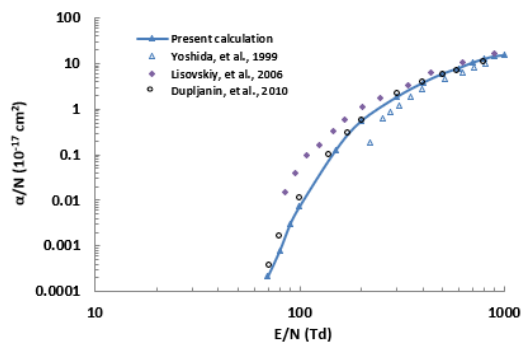

Figure 9. Reduced ionization coefficient α/N in N_2O.

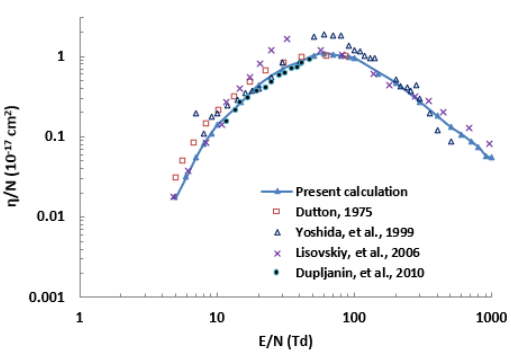

Figure 10. Reduced attachment coefficient η/N in N_2O.

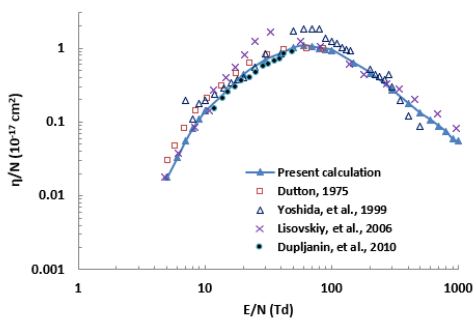

Figure 10. Reduced attachment coefficient η/N in N_2O.

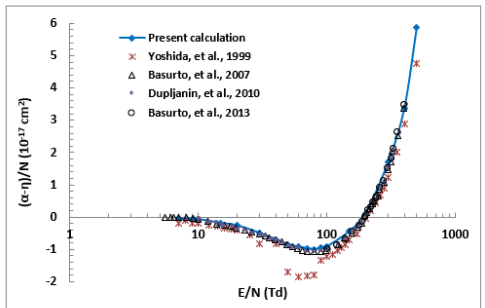

Figure 11. Reduced effective ionization coefficient (α-η)/N in N_2O.

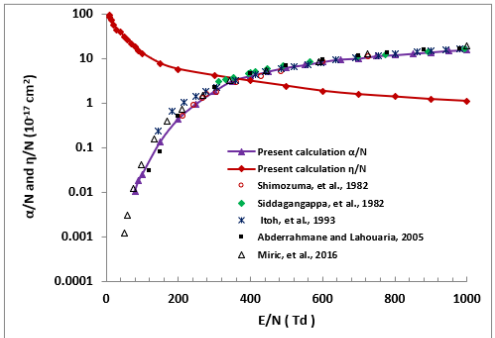

Figure 12. Reduced ionization coefficient α/N in SF_6.

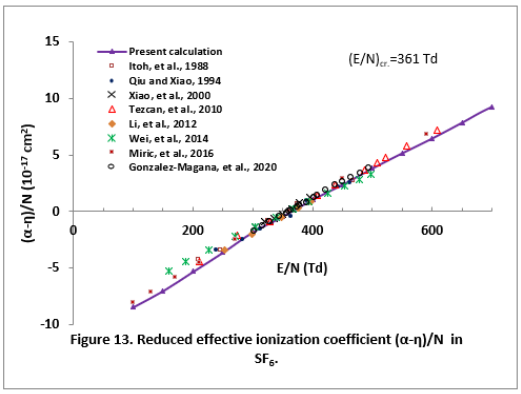

Figure 13. Reduced effective ionization coefficient (α-η)/N in SF_6.

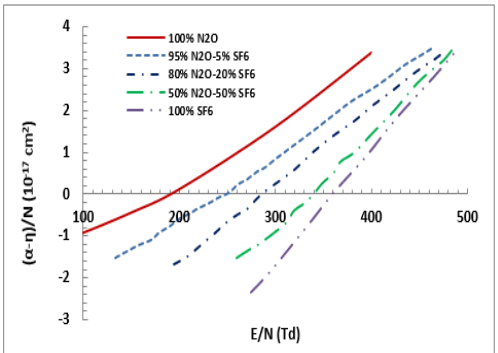

Figure 14. Reduced effective ionization coefficient (α-η)/N of N_2O-SF_6 mixtures for different SF_6 content.

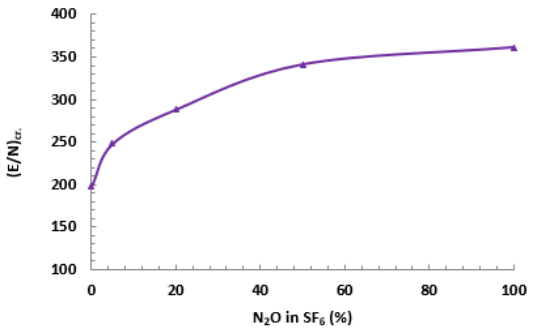

Figure 15. Critical reduced electric field strength of $(E/N)_{cr.}$ of N_2O-SF_6 as a function of SF_6 content.

5. CONCLUSION

The electron swarm parameters, namely (drift velocity, electron mean energy, characteristic energy, ionization and attachment coefficients), density-reduced effective ionization coefficient $(\alpha - \eta)/N$ and density-normalized critical field strength in pure N_2O, SF_6 and binary N_2O-SF_6 mixtures have been calculated using two term spherical harmonic approximation of the Boltzmann equation analysis at temperature 300 K and pressure 1 atm. The overall E/N is from 0.1 to 1000 Td, while the N_2O content in the binary N_2O-SF_6 mixtures can be varied from 100% to 0%. From the zeroth value of density-reduced effective ionization coefficient $(\alpha - \eta)/N$, the density-normalized critical field strength $(E/N)_{cr}$ for pure gases N_2O (199 Td), SF_6 (361 Td), and for each N_2O concentration is derived. The critical field strength increase with increasing SF_6 concentration in the gas mixtures.

6. REFERENCES

[1]. Akbar, M., and Malik, N. H. (1985). Electrical breakdown of N2O-SF6, N2O-CCl2F2 and N2O-CO2 gas mixtures, IEEE Transactions on Electrical Insulation, 3(3), pp. 581-585.

[2]. Andreas H., Juriy, P., Edda, E., Alise, C., Christian M. F. (2020). Measurement and modeling of electron and anion kinetics in N2O discharges, Journal of Physics D: Applied Physics 53(13), pp. 1-19.

[3]. E. Basurto, J.L. Hernández-Ávila, UA. M. Juárez P, J. de Urquijo P, S. Dupljanin, O. Šašić and Z. Lj. Petrović. (2007). Electron drift velocity and effective ionization coefficients in N2O, N2O-N2 and N2O-SF6, 28th ICPIG, July 15-20, Prague, Czech Republic.
[4]. Basurto, E., Hernad´ndez-Avila, J. L., Jua´rez, A. M., and de Urquijo, J. (2013). Electron swarm coefficients and the limiting field strength of SF6–N2O mixtures, J. Phys. D: Appl. Phys. 46(35), 355207 (7pp).
[5]. Biasiutti, G. (2013). Homogeneous field breakdown strength characteristics of some dielectric gases, Gaseous Dielectrics III. Elsevier, pp. 174-182.
[6]. Colonna, G., &D'Angola, A. (2016). Plasma Modeling; Methods and Applications. Plasma Modeling; Methods and Applications,. Bristol, UK: IOP Publishing.
[7]. Christophorou, L. G., and Brunt, R. J. V. (2002). SF6-N2 mixtures: basic and HV insulation properties, IEEE Transactions on Dielectrics and Electrical Insulation, 2(5), pp. 952–1003.
[8]. Dupljanin S, de Urquijo J, ˇSaˇsi´c O., Basurto E, Ju´arez A M, Herna´ndez-A´ vila J L, Dujko S and Petrovic´ Z Lj 2010 Transport coefficients and cross sections for electrons in N2O and N2O-N2 mixtures, Plasma Sources Sci. Technol., 19(2), 025005(9pp).
[9]. Dutton J, Harris F M and Hughes D B 1973 Electrical breakdown of nitrous oxide, Proc. IEE 120(8), pp. 941-444.
[10]. Gonz´alez-Magaña, O., Colorado, N. R., Basurto, E, Serkovic-Loli, L. N., Ju´arez1, A. M., Hern´andez-´Avila, J. L., and de Urquijo1, J. (2020). Electron swarm coefficients and critical field strength of the gaseous ternary mixtures CF3I-SF6-N2 and CF3I-SF6-CO2, J. Phys. D: Appl. Phys. 53 (18) 185203 (9pp).
[11]. Govinda-Raju, G. R. (2006). Gaseous Electronics: Theory and practice, Taylor and Francis LLc, Boca Raton, USA.
[12]. Gunnar, M. et al., (2013). Anthropogenic and natural radiative forcing. In: Climate change 423, pp. 658-740.
[13]. Hainan, Liu, (2020). Theoretical study of electron collisions with NO2 and N2O molecules for control and reduction of atmospheric pollution, PhD, thesis, University of Paris-Saclay.
[14]. Kim, K. T., Yoon, S. G., Yoon, S. G., Yung, S. G., Suh, S. J., Yoon, D. H. (2004). Plasma reactions of N2O on hydrogenated amorphous carbon films by PECVD, Surf. Coat. Technol., 180-181. pp. 250- 264.
[15]. Li, X., Zhao, H., and Jia, S. (2012). Dielectric breakdown properties of SF6–N2 mixtures in the temperature range 300–3000K, J. phys. D: Appl. Phys., 45(6), 445202(7pp).
[16]. Lisovskiy, V., P Booth, J., Landry, K., Douai, D., Cassagne, V., and Yegorenkov, V. (2006). Electron drift velocity in N2O in strong electric fields determined from rf breakdown curves, J. Phys. D: Appl. Phys., 39(9), pp.1866–1871.
[17]. Mechlinska-Drewko, J., Wroblewski, T., Petrovic, Z. Lj, Novakovic, V., and Karwasz, G. P. (2003). Electron scattering on N2O-from cross sections to diffusion coefficients, Radiat. Phys. Chem., 68(1-2), PP. 205-209.
[18]. Mirić, j., Bošnjaković, D., Simonović, I., Petrović, Z. Li., and Dujko, S. (2016). Electron swarm properties under the influence of a very strong attachment in SF6 and CF3I obtained by Monte Carlo rescaling procedures, Plasma Sources Sci. Technol., 25 (6) 065010 (15pp).
[19]. Tezcan, S. S., Ali Akcayol, M., Ozerdem, O. C. and M. S. Dincer, M. S. (2010). Calculation of Electron energy distribution functions from electron swarm parameters

using Artificial Neural Network in SF6 and Argon, IEEE Transaction on Plasma Science, 38(9), pp. 2332-2339.

[20]. Tuan, D. A. (2016). Analysis of electron transport coefficients in binary mixtures of TEOS gas with Kr, Xe, He and Ne gases for using in plasma assisted thin-film deposition. Journal of Electrical Engineering and Technology, 11(2), pp. 455-462.

[21]. Wei, L., Xu, M., Yuan, D., Zhang, Y., Hu, Z., and Tan, Z. (2014). Electron transport Coefficients and effective ionization coefficients in SF6-O2 and SF6-air mixtures using Boltzmann analysis, Plasma Science and Technology, 16(10), pp. 941-947.

[22]. Xiao, D. M., Zhu, L. L., and Li, X. G. (2000). Electron transport coefficients in SF6 and xenon gas mixtures, J. phys. D: Appl. Phys., 33(23), L145-L147.

[23]. Zhao, H., Li, X., Jia, S., & Murphy, A. B. (2013). Dielectric breakdown properties of SF6–N2 mixtures at 0.01–1.6 MPa and 300–3000 K. Journal of Applied Physics, 113(14), 143301(6pp).

[24]. Ganesh Babu Loganathan, Praveen M., Jamuna Rani D., "Intelligent classification technique for breast cancer classification using digital image processing approach" IEEE Xplore Digital Library 2019, Pp.1-6.

[25]. M. Viswanathan, Ganesh Babu Loganathan, and S. Srinivasan, "IKP based biometric authentication using artificial neural network", AIP Conference Proceedings (2020), Volume 2271, Issue 1, pp 030030.

[26]. Mohammed Abdulghani Taha and Ganesh Babu Loganathan, "Hybrid algorithms for spectral noise removal in hyper spectral images" AIP Conference Proceedings (2020), Volume 2271, Issue 1, pp 030013.

[27]. Dr.IdrisHadiSalih, Ganesh Babu Loganathan, "Induction motor fault monitoring and fault classification using deep learning probablistic neural network" Solid State Technology(2020), Volume 63, Issue 6, PP No. 2196-2213.

[28]. Ganesh Babu Loganathan "Design and analysis of high gain Re Boost-Luo converter for high power DC application", Materials Today: Proceedings(2020), Volume 33, Part 1, PP 13-22.

[29]. Ganesh BabuLoganathan, Dr.E.Mohan, R.Siva Kumar, " Iot Based Water And Soil Quality Monitoring System", International Journal of Mechanical Engineering and Technology (IJMET)(2019), Vol.10 Issue No.2, P.No. 537-541.

[30]. Suganthi K, IdrisHadi Salih, Ganesh BabuLoganathan, and Sundararaman K, "A Single Switch Bipolar Triple Output Converter with Fuzzy Control", International Journal of Advanced Science and Technology, (2020), Vol. 29, No. 5, (2020), P.No.. 2386 – 2400.

[31]. Ganesh Babu Loganathan, "Can Based Automated Vehicle Security System", International Journal of Mechanical Engineering and Technology (IJMET)(2019), Vol.10 Issue No.07, P.No. 46-51.

[32]. Loganathan, Ganesh Babu, Vanet Based Secured Accident Prevention System (September 10, 2019). International Journal of Mechanical Engineering and Technology, 10(6), 2019, pp. 285-291, Available at SSRN: https://ssrn.com/abstract=3451201

[33]. B.K. Patle, Ganesh Babu L, AnishPandey, D.R.K. Parhi, A. Jagadeesh,A review: On path planning strategies for navigation of mobile robot, Defence Technology, Volume 15, Issue 4, August 2019, Pages 582-606.

[34]. R. Sujith Kumar, G. Swaminathan, Ganesh Babu Loganathan, "Design and analysis of composite belt for high rise elevators" ,Materials Today: Proceedings, Volume 22, Part 3, 2020, Pages 663-672, ISSN 2214-7853,

[35]. Dr.A.Senthil Kumar, Dr.Venmathi A R ,L.GaneshBabu, Dr.G. Suresh, "Smart Agriculture Robo With Leaf Diseases Detection Using IOT", European Journal of

Molecular & Clinical Medicine, Volume 07, Issue 09, PP 2462-2469.
[36]. Ganesh Babu L 2019 Influence of benzoyl chloride treatment on the tribological characteristics of Cyperuspangorei fibers based nonasbestos brake friction composites Mater. Res. Express 7 015303.
[37]. Sivam, S.P.S.S., Loganathan, G.B., Kumaran, D., Saravanan, K., Rajendra Kumar, S., 2019. Performance Evaluation of Yield Function and Comparison of Yielding Characteristics of SS 304 in Annealed and Unannealed Conditions. MSF 969, 637–643. https://doi.org/10.4028/www.scientific.net/msf.969.637
[38]. A.Devaraju, P.Sivasamy, Ganesh BabuLoganathan, "Mechanical properties of polymer composites with ZnOnano-particle" , Materials Today: Proceedings(2020), Volume 22, Part 3, Pages 531-534
[39]. QaysarS.Mahdi, "Prediction of Mobile Radio Wave Propagation in Complex Topography" , Eurasian Journal of Science & Engineering, Volume 4, Issue 1 (Special Issue); September, 2018, PP 49-55.
[40]. Qaysar S. Mahd, "Survivability Analysis of GSM Network Systems", Eurasian Journal of Science & Engineering, Volume 3, Issue 3;June, 2018, PP 113-123.
[41]. QaysarS.Mahdi, "Comparison Study of Multi-Beams Radar under Different Radar Cross Section and Different Transmitting Frequency", Eurasian Journal of Science & Engineering, Volume 3, Issue 3; June, 2018, PP 1-11.
[42]. Ellappan Mohan, Arunachalam Rajesh , Gurram Sunitha , Reddy Madhavi Konduru , Janagaraj Avanija, Loganathan Ganesh Babu, "A deep neural network learning-based speckle noise removal technique for enhancing the quality of synthetic-aperture radar images", Concurrency And Computation-Practice & Experience, https://doi.org/10.1002/cpe.6239.
[43]. Dr.A.Senthil Kumar, Dr.G.Suresh, Dr.S.Lekashri, Mr.L.GaneshBabu, Dr. R.Manikandan, "Smart Agriculture System With E – Carbage Using Iot", International Journal of Modern Agriculture, Volume 10, No.1, 2021 pp 928-931.
[44]. Ganesh BabuLoganathan, IdrisHadiSalih, A.Karthikayen, N. Satheesh Kumar, UdayakumarDurairaj. (2021). EERP: Intelligent Cluster based Energy Enhanced Routing Protocol Design over Wireless Sensor Network Environment. International Journal of Modern Agriculture, 10(2), 1725 - 1736. Retrieved from http://www.modern-journals.com/index.php/ijma/article/view/908
[45]. BABU LOGANATHAN, ganesh; E.MOHAN, Dr.. High Quality Intelligent Database Driven Microcontroller Based Heartbeat Monitoring System. International Journal of Engineering & Technology, [S.l.], v. 7, n. 4.6, p. 472-476, sep. 2018. ISSN 2227-524X.
[46]. Muthuramalingam, T., Saravanakumar, D., Babu, L.G. *et al.* Experimental Investigation of White Layer Thickness on EDM Processed Silicon Steel Using ANFIS Approach. *Silicon* 12, 1905–1911 (2020). https://doi.org/10.1007/s12633-019-00287-2
[47]. G, Sai Krishnan and Loganathan, Ganesh Babu and K, Selva Ganapathy and N, Srivathsan and M, Vasanth and G, Venkatateja, Development of Superhydrophobic Nanocomposite Coatings on FRP Sheet Surface for Anti-Icing and Wear-Resistance Applications (August 5, 2019). Proceedings of International Conference on Recent Trends in Computing, Communication & Networking Technologies (ICRTCCNT) 2019, Available at SSRN: https://ssrn.com/abstract=3432305 or http://dx.doi.org/10.2139/ssrn.3432305
[48]. S.P. Sundar Singh Sivam, Ganesh BabuLoganathan, K. Saravanan, S. RajendraKumar, "Outcome of the Coating Thickness on the Tool Act and Process Parameters When Dry Turning Ti–6Al–4V Alloy: GRA Taguchi & ANOVA", International Journal of

Innovative Technology and Exploring Engineering (IJITEE) ISSN: 2278-3075, Volume-8, Issue-4, February 2019 PP. 419-423.

[49]. SivamSundarlingamParamasivam, S., Loganathan, G., Kumaran, D., Saravanan, K. et al., "Function of Taguchi Grey Relation Analysis for Influencing the Process Parameter for Getting Better Product Quality and Minimize the Industrial Pollution by Coolants in Turning of Ti-6Al-4V Alloy," SAE Technical Paper 2019-28-0065, 2019, https://doi.org/10.4271/2019-28-0065.

[50]. Sivam S.P.S.S., Loganathan G.B., Saravanan K., Dinesh Guhan S., Banerjee A. (2021) Effects of Drilling Process Parameters Using ANOVA and Graphical Methods. In: Kumaresan G., Shanmugam N.S., Dhinakaran V. (eds) Advances in Materials Research. Springer Proceedings in Materials, vol 5. Springer, Singapore. https://doi.org/10.1007/978-981-15-8319-3_35

[51]. Muthuramalingam T., Ganesh Babu L., Sridharan K., Geethapriyan T., Srinivasan K.P. (2020) Multi-response Optimization of WEDM Process Parameters of Inconel 718 Alloy Using TGRA Method. In: Sattler KU., Nguyen D., Vu N., Tien Long B., Puta H. (eds) Advances in Engineering Research and Application. ICERA 2019. Lecture Notes in Networks and Systems, vol 104. Springer, Cham. https://doi.org/10.1007/978-3-030-37497-6_56

[52]. BABU, L. G. (2020). Influence on the tribological performance of the pure synthetic hydrated calcium silicate with cellulose fiber. In *Journal of the Balkan Tribological Association* (Vol. 26, Issue 4, pp. 747–754).

[53]. Sai Krishnan G., Shanmugasundar, Pradhan R., Loganathan G.B. (2020) Investigation on Mechanical Properties of Chemically Treated Banana and Areca Fiber Reinforced Polypropylene Composites. In: Praveen Kumar A., Dirgantara T., Krishna P.V. (eds) Advances in Lightweight Materials and Structures. Springer Proceedings in Materials, vol 8. Springer, Singapore. https://doi.org/10.1007/978-981-15-7827-4_27

[54]. Dr. Kapila Uma Shankar, Dr. Waqar Ahmad, SallarAshqi Kareem, “beta volatility and its consequences for hedging systematic risk with reference to stock market during covid-19”, Information Technology in Industry, Volume 09, Issue 03,2021, 482 – 492.

[55]. Dr. Uma Shankar, “Debt Restructuring to Elongate Asset Quality of Banks In India”, Solid State Technology (2020), Volume 63, Issue 6, PP No. 14540-14549

[56]. Dr.Kapila Uma Shankar, “Analysis on Social Banking for Sustainable Growth and Satisfaction on Social Targets”, International Journal of Advanced Science and Technology, Volume 29, Issue 7, PP No. 14487-14491.

[57]. P.Govindasamy ,Kapila Uma Shankar, “Covid-19 And Global Financial Markets With Special Focus To Gdp Growth Projection, Capital Mobilization And Performance Of Stock Market” Volume XI, Issue VII, 2020, PP No. 1-9.

[58]. Dr. Uma Shankar. (2021). Impact of Quantitative Easing on Economic Crisis During Pandemic. International Journal of Modern Agriculture, 10(2), 3342 - 3350. Retrieved from http://www.modern-journals.com/index.php/ijma/article/view/1168

[59]. Dr. Uma Shankar. (2021). Influence of Financial Statement Comparability on Applicability of Earnings. *International Journal of Modern Agriculture*, *10*(2), 3323 - 3332.Retrievedfromhttp://www.modernjournals.com/index.php/ijma/article/view/1166

[60]. Dr.P. Govindasamy; Dr.Kapila Uma Shankar; Mr.R. Ravimohan. "Indian capital market analysis 2020 year end and 2021 year beginning". Journal of Contemporary Issues in Business and Government, *27, 2, 2021, 6677-6693.* doi: 10.47750/cibg.2021.27.02.645

[61]. Dr. Othman, M.M., Ishwarya, K.R., Ganesan, M. and Babu Loganathan, G. (2021). A Study on Data Analysis and Electronic Application for the Growth of Smart Farming.

Alinteri Journal of Agriculture Sciences, 36(1): 209-218. doi: 10.47059/alinteri/V36I1/AJAS21031.